OPEN ACCESS
CellPress

Cell Reports
Report

Rif1 Controls DNA Replication Timing in Yeast through the PP1 Phosphatase Glc7

Stefano Mattarocci,[1,5] Maksym Shyian,[1,5] Laure Lemmens,[1] Pascal Damay,[1] Dogus Murat Altintas,[1] Tianlai Shi,[2,4] Clinton R. Bartholomew,[3] Nicolas H. Thomä,[2] Christopher F.J. Hardy,[3] and David Shore[1,*]

[1]Department of Molecular Biology and Institute of Genetics and Genomics in Geneva, University of Geneva, 30 quai Ernest-Ansermet, 1211 Geneva, Switzerland
[2]Friedrich Miescher Institute for Biomedical Research, Maulbeerstrasse 66, 4058 Basel, Switzerland
[3]Department of Cell and Developmental Biology, Vanderbilt University Medical Center, T-2212 Medical Center North, Nashville, TN 37232-2175, USA
[4]Present address: Hoffmann-La Roche Ltd., 4070 Basel, Switzerland
[5]These authors contributed equally to this work
*Correspondence: david.shore@unige.ch
http://dx.doi.org/10.1016/j.celrep.2014.03.010

SUMMARY

The Rif1 protein, originally identified as a telomere-binding factor in yeast, has recently been implicated in DNA replication control from yeast to metazoans. Here, we show that budding yeast Rif1 protein inhibits activation of prereplication complexes (pre-RCs). This inhibitory function requires two N-terminal motifs, RVxF and SILK, associated with recruitment of PP1 phosphatase (Glc7). In G1 phase, we show both that Glc7 interacts with Rif1 in an RVxF/SILK-dependent manner and that two proteins implicated in pre-RC activation, Mcm4 and Sld3, display increased Dbf4-dependent kinase (DDK) phosphorylation in *rif1* mutants. Rif1 also interacts with Dbf4 in yeast two-hybrid assays, further implicating this protein in direct modulation of pre-RC activation through the DDK. Finally, we demonstrate Rif1 RVxF/SILK motif-dependent recruitment of Glc7 to telomeres and earlier replication of these regions in cells where the motifs are mutated. Our data thus link Rif1 to negative regulation of replication origin firing through recruitment of the Glc7 phosphatase.

INTRODUCTION

DNA replication in eukaryotes is initiated from specific chromosomal sites (origins), which fire in a temporal pattern during S phase that depends on cell type and developmental stage. The unfolding of this replication program is controlled through mechanisms that remain poorly understood to date. Recent studies show that premature firing of normally late or dormant origins in yeast can lead to activation of a DNA-damage response, most likely as a consequence of deoxynucleotide triphosphate depletion (Mantiero et al., 2011). This finding suggests that control of origin usage may be connected in some way to replication fork progression.

The control of DNA replication initiation is best understood in the budding yeast *Saccharomyces cerevisiae*, where, unlike in all other eukaryotes studied to date, potential replication origins, or autonomously replicating sequences (ARS), are well defined by a conserved sequence bound constitutively by the origin recognition complex (ORC) (Siddiqui et al., 2013). Origins are first prepared for replication through the loading of the replicative helicase (MCM2–MCM7 hexamer) to form the prereplication complex (pre-RC). Activation of the pre-RC requires the combined action of two kinase complexes, the cyclin-dependent kinase (CDK) and the Dbf4-dependent kinase (DDK), the latter consisting of the Cdc7 kinase and its activator Dbf4 (Labib, 2010), and is associated with the recruitment of additional proteins, including Cdc45, implicated in MCM2–MCM7 release during initiation; a set of adaptor proteins, Sld2/Sld3 and Dpb11; the GINS complex, containing four proteins implicated in polymerase assembly at the origin; and the leading strand DNA polymerase itself, Polε (Araki, 2011).

The temporal pattern of DNA replication during S phase in yeast has been extensively studied (Aparicio, 2013). In this organism, only a small fraction of potential origins actually fire early during S phase. Other origins fire during middle or late S phase or not at all and are thus passively replicated. Significantly, overexpression of several factors, particularly Sld2/Sld3, Dbf4, and Dpb11, accelerates initiation of normally late-firing origins, suggesting that the temporal pattern of initiation is entrained by a competition for limiting factors (Mantiero et al., 2011). Telomeres tend to replicate late in S phase (Donaldson, 2005), despite their proximity to nearby ARS elements, due to the action of two proteins involved in gene silencing at telomeres, Sir3 and the Ku heterodimer (Yku70/Yku80) (Cosgrove et al., 2002; Stevenson and Gottschling, 1999). More recent studies have shown that a third telomere-binding protein, Rif1, also determines late telomere replication (Lian et al., 2011). Mutation of *RIF1*, in addition to causing earlier telomere replication, also leads to elongation of $TG_{(1–3)}$ tract length at telomeres, yet paradoxically, in otherwise wild-type cells, short telomeric TG-repeat tracts entrain the linked telomere to replicate earlier (Bianchi and Shore, 2007). Taken together, these data implicate the telomere length

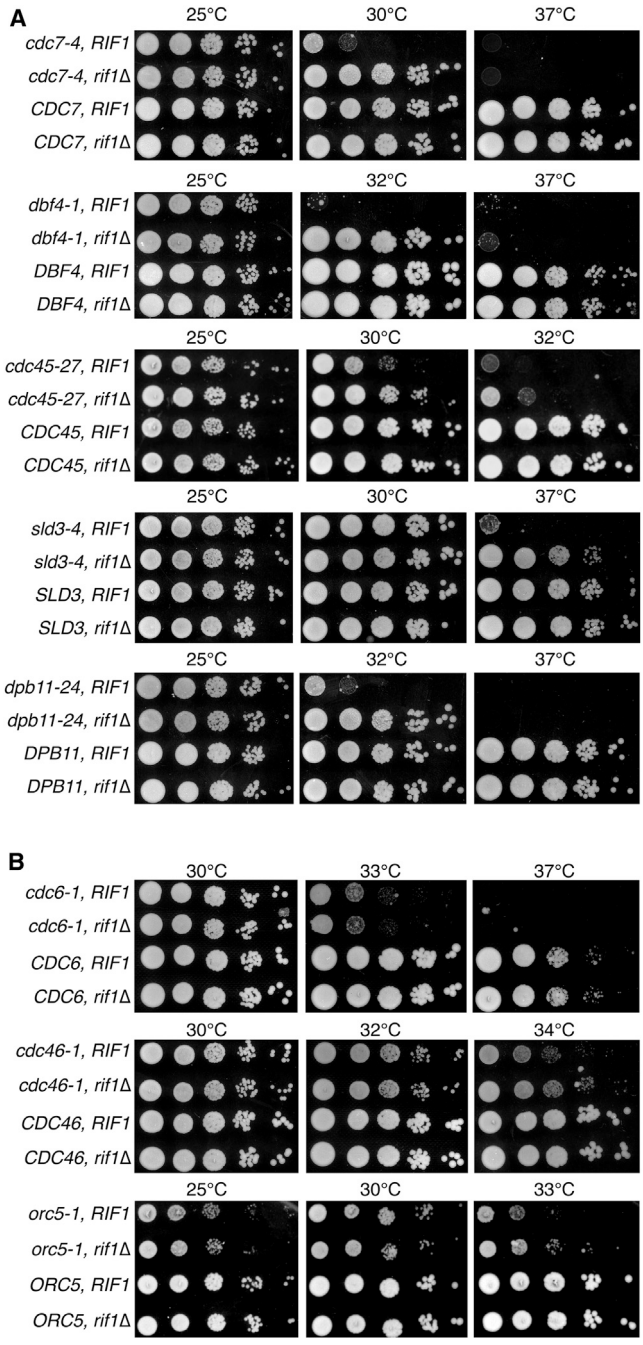

Figure 1. *RIF1* Deletion Suppresses Mutations Affecting DNA Replication Initiation

Temperature-sensitive (ts) replication mutants, together with either *RIF1* or *rif1Δ*, were grown overnight in rich medium (YPAD) at 25°C. Serial 10-fold dilutions were spotted onto YPAD plates and incubated at the indicated temperatures for 48 hr. In each panel, isogenic wild-type controls for the different ts mutants are shown. See also Figure S1.

regulatory mechanism and telomeric gene silencing in control of telomere-proximal origin firing, though the mechanisms involved remain obscure.

Here, we explore in molecular detail the role of Rif1 in telomere-replication timing and more generally in the regulation of genome-wide origin activation. Our findings suggest a model in which Rif1 affects replication initiation through recruitment of the PP1 phosphatase (Glc7), most likely at replication origins themselves, where it counteracts the effect of the DDK.

RESULTS

Rif1 Has a Global Effect on pre-RC Activation in Budding Yeast

The previous finding that deletion or knockdown of *RIF1* in yeast or mammalian cells leads to earlier DNA replication at some chromosomal sites suggests a role for Rif1 in directly regulating replication origin activation (Cornacchia et al., 2012; Hayano et al., 2012; Lian et al., 2011; Yamazaki et al., 2012). In support of this notion, studies in the fission yeast *Schizosaccharomyces pombe* showed that deletion of *RIF1* can rescue the lethality of an *hsk1*$^+$ deletion, which removes the essential DDK required for replication initiation (Hayano et al., 2012). We found a similar effect of *RIF1* deletion in a *Saccharomyces cerevisiae* strain carrying a *cdc7-4* temperature-sensitive (ts) mutation (*CDC7* is the budding yeast ortholog of *hsk1*$^+$) but noted that *rif1Δ* does not completely bypass the requirement for Cdc7, because *rif1Δ cdc7-4* cells still do not grow at 37°C (Figure 1A), and *rif1Δ* does not permit growth of cells deleted for *CDC7* (data not shown).

To ask whether the action of *RIF1* is specific to *CDC7*, we examined the effect of *rif1Δ* on other factors required for pre-RC activation, again using temperature-sensitive alleles of the corresponding (essential) genes. Notably, we found that *rif1Δ* strongly suppressed *dbf4-1*, *sld3-4*, and *dpb11-24* mutations, whereas it displays a more modest effect on *cdc45-27*, encoding a third activation factor (Figure 1A). In contrast, the influence of *rif1Δ* on alleles affecting the helicase or its loading onto origins (*cdc46-1*, *orc5-1*, and *cdc6-1*) was either minimal or undetectable (Figure 1B). This analysis suggests that Rif1 has an inhibitory effect related to the DDK and three pre-RC activator proteins (Cdc45, Sld3, and Dpb11), whereas relatively little or no effect on pre-RC assembly (e.g., Cdc6 and Cdc46/Mcm5).

The fact that late-firing origins are controlled by limiting amounts of some pre-RC activation factors (Mantiero et al., 2011; Tanaka et al., 2011) raises the possibility that the suppression effect we observe for *rif1Δ* might result from an increase in the amount of one or more of these proteins. However, we found no evidence for this (Figure S1). Although we cannot rule out a small abundance change that could have phenotypic consequences, we present data below showing that at least two initiation factors, including Sld3, display increased phosphorylation in *rif1Δ* cells.

Conserved RVxF- and SILK-like Motifs in Rif1 Mediate Its Effect on Pre-RC Activation

To address the mechanism of Rif1 inhibition of pre-RC activity, we initiated a structure-function analysis. Rif1 is a large protein with a long, centrally located array of helical repeats and a C-terminal domain required for telomere binding through interactions with Rap1 (Shi et al., 2013). Deletion of the C-terminal domain

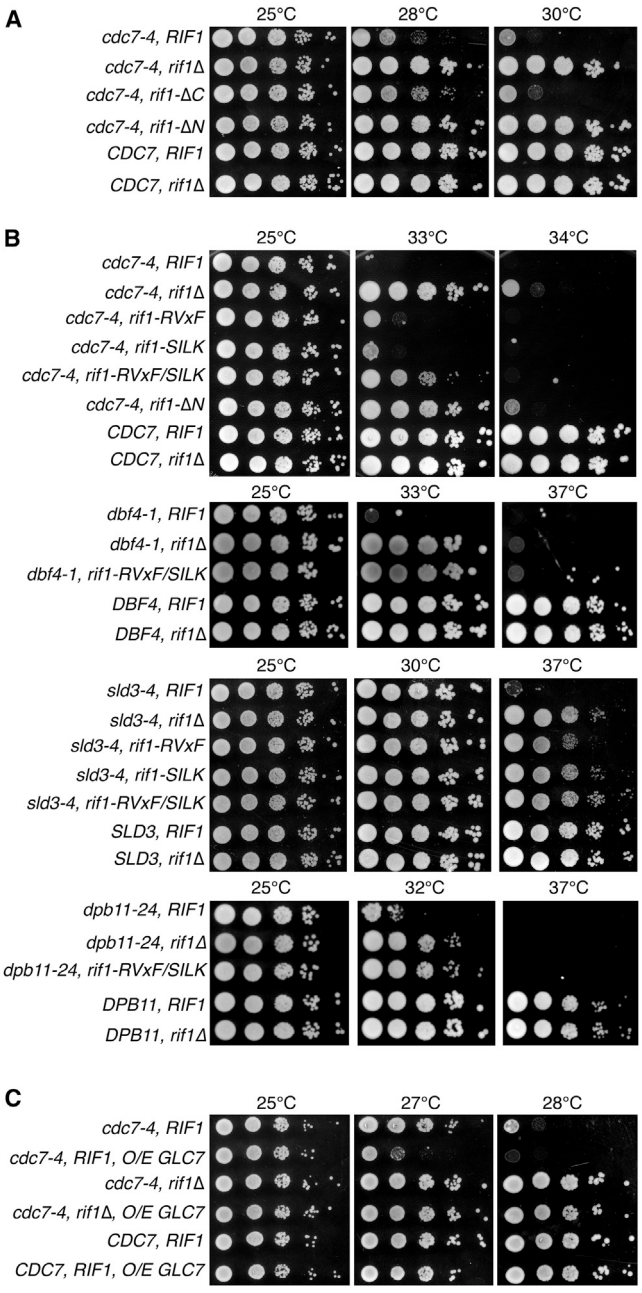

Figure 2. Glc7 Interaction Motifs in Rif1 and *GLC7* Dosage Modulate DNA Replication Initiation

(A and B) Cells with the indicated genotypes (*rif1-RVxF* and *rif1-SILK* cells carry point mutations in, respectively, RVxF and SILK motifs) were assayed as described in Figure 1.

(C) Cells with the indicated genotypes carrying either an empty plasmid or a plasmid containing the *GLC7* gene (p*GLC7*) were grown overnight in liquid medium lacking uracil (SC-Ura) at 25°C. Serial 10-fold dilutions were spotted onto SC-Ura plates and incubated at indicated temperatures for 48 hr.

See also Figure S2.

(from residue 1323 to the end at 1916) had no effect on growth of a *cdc7-4* mutant (Figure 2A). In contrast, an N-terminal deletion (residues 2–176; *rif1-ΔN*) resulted in strong suppression of *cdc7-4,* similar to that observed for *rif1Δ* (Figures 2A and 2B). The yeast Rif1 N terminus was shown recently to contain two short peptide motifs (commonly abbreviated as RVxF/SILK and referred to as such here, but actually KSVAF/SILR in *S. cerevisiae*; Sreesankar et al., 2012) that have been associated with recruitment of the PP1 phosphatase (Hendrickx et al., 2009), encoded by *GLC7* in yeast. PP1 (Glc7) is an abundant, highly conserved serine/threonine phosphatase that controls many different processes in all eukaryotic cells (Cannon, 2010). Interestingly, these motifs are conserved in fly and mammalian Rif1 homologs, though their position within the protein and their orientation are not. We generated point mutations in these two motifs and introduced them individually or in combination at the endogenous *RIF1* locus.

Strikingly, the combined RVxF/SILK domain mutations suppressed the *cdc7-4*, *dbf4-1*, *sld3-4*, and *dpb11-24* growth defects as well (or nearly, in the case of *cdc7-4*) as *rif1Δ* (Figure 2B). Where we examined either RVxF or SILK mutations alone (in *cdc7-4* and *sld3-4* strains), suppression was evident but weaker, indicating that the two motifs have an additive effect. We observed a similar effect of RVxF/SILK mutation on growth of *cdc45-27* (Figure S2A) and showed that the ΔN, RVxF, and SILK mutations do not act by reducing Rif1 protein levels (Figure S2B). Despite the fact that *rif1-ΔN* cells show a clear increase in Rif1 protein level compared to wild-type (Figure S2B), this mutation, lacking the two Glc7 interaction motifs, suppresses the *cdc7-4* growth defect as well as *rif1Δ* (Figure 2B).

If the RVxF/SILK mutations improved growth of *cdc7-4* by decreasing Glc7 recruitment at origins, overexpression of Glc7 might be expected to have the opposite effect. Indeed, we found that modest overexpression of Glc7 is sufficient to reduce the permissive temperature of a *cdc7-4* mutant (Figure 2C) but that this effect is abolished by *rif1Δ*. Taken together, these data strongly suggest that Glc7 acts downstream of Rif1 in the inhibition of origin firing.

Rif1 Interacts with Both Glc7 and Dbf4 and Regulates the Phosphorylation of Mcm4 and Sld3

The results described above suggest that Rif1 affects pre-RC activation through recruitment of the Glc7 phosphatase, which in turn directly counteracts the effect of DDK (and perhaps CDK) at replication origins. To test this idea, we first asked whether Rif1 and Glc7 physically interact in cells. We immunoprecipitated FLAG epitope-tagged Glc7 protein (expressed from the native *GLC7* locus) and probed the precipitate for Rif1-Myc (also expressed from the endogenous locus). As shown in Figure 3A, Rif1-Myc is enriched in precipitates from Glc7-FLAG-expressing G1-arrested cells, and this binding is strongly decreased in cells expressing the rif1-RVxF/SILK-Myc mutant protein (see also Figure S3A for two independent experiments and a coimmunoprecipitation [co-IP] in which the epitope tags were reversed).

We next asked whether Rif1 has an effect on the phosphorylation state of the pre-RC or its activators by focusing on a well-established DDK target, the MCM helicase component Mcm4 (Sheu and Stillman, 2006). We first examined Mcm4-Myc protein mobility by SDS-PAGE in extracts from *RIF1*, *rif1Δ*, and *rif1-RVxF/SILK* cells arrested either in G1 (following treatment with

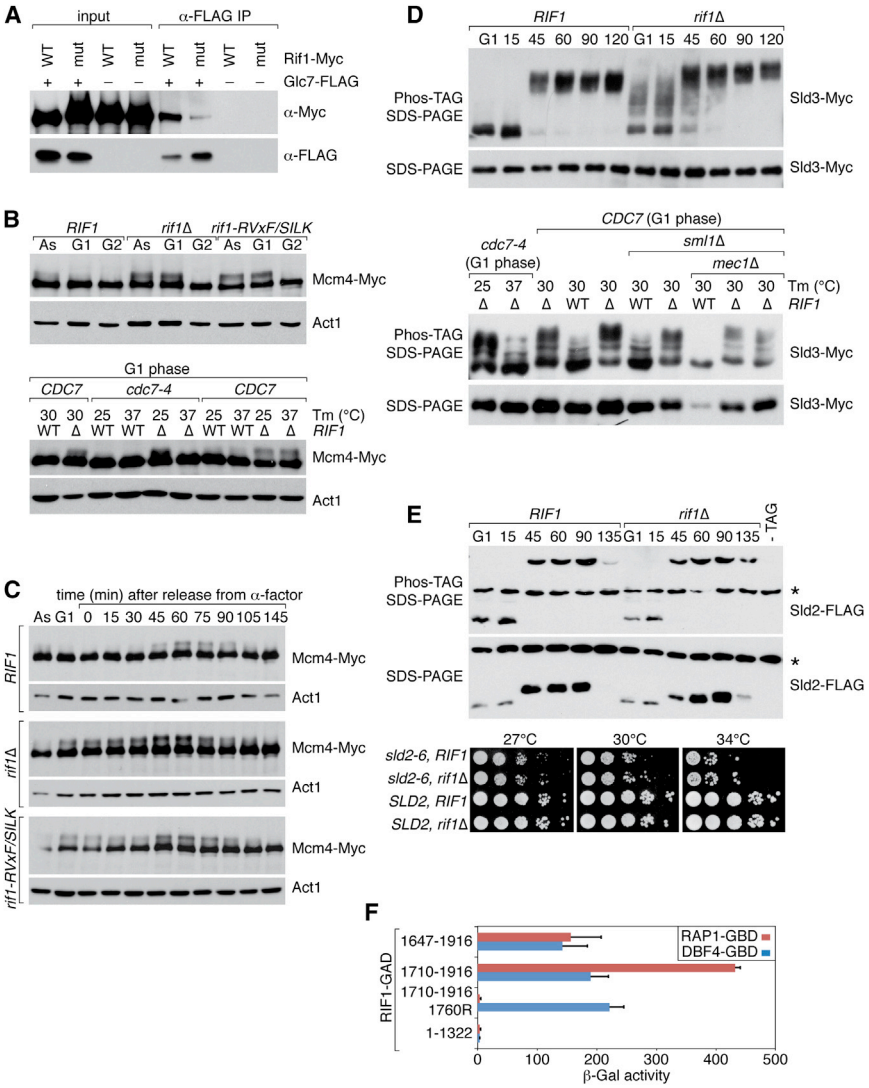

Figure 3. Rif1 Interacts with Both Glc7 and Dbf4 and Regulates the DDK-Dependent Phosphorylation of the Replicative Helicase Protein Mcm4 and the Pre-RC Activator Sld3

(A) Western blot using a Myc monoclonal antibody (mAb) following immunoprecipitation with anti-FLAG M2 beads from cells expressing Glc7-FLAG and either Rif1-Myc (WT) or rif1-RVxF/SILK-Myc (mut) or from control cells expressing only Rif1-Myc or rif1-RVxF/SILK-Myc. Extracts were prepared from G1-arrested cells. The same samples were analyzed by western blot using FLAG antibody.

(B) *RIF1*, *rif1–RVxF/SILK*, and *rif1Δ* cells, all of which express a Mcm4-Myc protein from the endogenous *MCM4* locus, were arrested either in G1 or G2 phase by α factor or nocodazole (10 μg/ml) treatments, respectively. Protein extracts were prepared and analyzed by western blot with a Myc mAb and with actin antibody as a loading control. As, asynchronous culture (top panel). *CDC7* or *cdc7-4* cells expressing Mcm4-Myc were grown at 25°C and then shifted to the indicated temperatures in the presence of α factor for 2 hr. Western blots were carried out as above (bottom panel).

(C) The strains described in (B, top panel) were arrested in G1 phase and then released into a synchronous S phase at 18°C. Protein extracts were prepared at the indicated times following release from the G1 block and analyzed by western blot using Myc and actin antibodies.

(D) Phos-tag SDS-PAGE western blots of extracts from either *RIF1* or *rif1Δ* cells probed for Sld3-Myc (expressed from the endogenous *SLD3* locus). Cells were G1-arrested and released into a synchronous S phase at 18°C. Aliquots were taken at the indicated time points. The same samples were analyzed by standard SDS-PAGE western blot as a measure of total Sld3 protein (top panel). Cells of the indicated genotypes, all expressing Sld3-Myc, were grown at 25°C and then shifted to the indicated temperatures in the presence of α factor for 2 hr. Western blots were carried out as above (bottom panel).

(E) Phos-tag and normal SDS-PAGE western blot using FLAG mAb of extracts from either *RIF1* or *rif1Δ* cells expressing Sld2-FLAG from the endogenous *SLD2* locus. Cells were G1-arrested and released as in (D, top panel; top panel; *, nonspecific band). Cells with the indicated genotypes were grown and spotted in YPAD plates as indicated in Figure 1 (bottom panel).

(F) Two-hybrid assays in a *rif1Δ* derivative of the PJ69-4a reporter strain were performed using GBD-Dbf4 or GBD-Rap1 fusions as "bait" with indicated GAD-Rif1 fragments "prey." The β-galactosidase activity levels reported are averages (with SD) of at least two independent biological replicates.

See also Figure S3.

mating pheromone) or G2/M (by nocodazole treatment). This preliminary analysis revealed a prominent slower-mobility species specific to both G1-arrested *rif1Δ* and *rif1-RVxF/SILK* mutant cells (Figure 3B, top panel) that is abolished by phosphatase treatment (data not shown) and absent when cdc7-4 protein is inactivated (Figure 3B, bottom panel; 37°C). To examine Mcm4 phosphorylation in more detail, we monitored cells released from G1 arrest into a synchronous S phase. As shown in Figure 3C, and consistent with the previous experiment, we detected a modified form of Mcm4 only in G1-arrested *rif1Δ* and *rif1-RVxF/SILK* mutant cells, which increased in intensity and reached a maximum at the 60 min time point but was undetectable at 90 min, when S phase was completed (as shown by fluorescence-activated cell sorting [FACS] analysis and Clb2 accumulation; see Figure S3B, left panels). Interestingly, wild-type (*RIF1*) cells showed no evidence for Mcm4 phosphorylation at early times (0–30 min following release from G1) but displayed a slower-mobility species starting at 45 min (when early ARSs are fired, as measured by RPA recruitment; see Figure S3B, right panel) and increasing at 60 and 75 min, similar to that observed in the *rif1Δ* cells (Figure 3C; for a separate experiment in which samples were loaded on one gel, see Figure S3C).

We also examined the phosphorylation state of two well-known CDK targets, Sld2 and Sld3 (Tanaka et al., 2007;

Zegerman and Diffley, 2007), using a Phos-tag gel to enhance the mobility shift of phosphorylated protein (see Experimental Procedures). We observed a prominent mobility shift in Sld3-Myc from G1 phase cells, and until 30 min following G1 release, that was specific for the *rif1Δ* mutant (Figure 3D, top panel; Figure S3D, left panel). As both *RIF1* and *rif1Δ* cells enter S phase at 45 min, Sld3 becomes highly phosphorylated (Figure 3D, top panel; Figure S3D, left panel), which previous studies have shown to result from S phase CDK action (Tanaka et al., 2007; Zegerman and Diffley, 2007). Total Sld3 levels are similar in these strains, indicating that the early-stage appearance of the shifted Sld3 band is not due to increased Sld3 expression in the *rif1Δ* mutant. Because the S phase CDK is not active in G1 cells, we asked whether Sld3 phosphorylation might require Cdc7 activity. We also examined the Mec1 kinase, which had previously been implicated in Sld3 phosphorylation (Lopez-Mosqueda et al., 2010; Zegerman and Diffley, 2010). Interestingly, we found that the G1-specific phosphorylation of Sld3 in *rif1Δ* cells is abolished when cdc7-4 protein is inactivated (37°C sample) but unaffected by the absence of Mec1 (Figure 3D, bottom panel; Figure S3D, right panel). These data suggest that, as for the case of Mcm4, Sld3 is targeted by the DDK in G1 but that this phosphorylation is strongly counteracted by Rif1-Glc7. Interestingly, identical experiments in cells expressing Sld2-FLAG show no difference between *RIF1* and *rif1Δ* cells in the mobility of this protein either in G1 or as cells enter and proceed through S phase, where the protein becomes highly modified (Figure 3E, top panel). Consistent with this absence of Rif1-dependent phosphorylation of Sld2, we found that an *sld2-6* mutant is not suppressed by *rif1Δ* (Figure 3E, bottom panel). Another target of CDK, Orc6 (Chen and Bell, 2011), shows no change in its phosphorylation status between *RIF1* and *rif1Δ* cells (Figure S3E). Taken together, these data suggest that the action of Rif1-Glc7 might be limited to G1 phase and to DDK targets (Mcm4 and Sld3, though perhaps others).

In the course of investigating the role of Dbf4 in DNA replication initiation, we performed a yeast two-hybrid screen using full-length Dbf4 as bait and identified a C-terminal portion of Rif1 (amino acids 1647–1916) as an interacting polypeptide (Figure 3F). Interestingly, a nearly identical clone of *RIF1* was originally identified through its two-hybrid interaction with a C-terminal domain of Rap1 (Hardy et al., 1992). More recently, we demonstrated a direct interaction between a short α-helical region within the Rif1 C terminus ($Rif1_{RBM}$, amino acids 1752–1772) and a conserved groove in the Rap1 C terminus (Shi et al., 2013). Mutation of a critical residue within this peptide abolishes the interaction with Rap1, as shown before (Shi et al., 2013), but has no effect on the interaction with Dbf4 (Figure 3F). The experiments shown in Figure 3F were all performed in a *rif1Δ* reporter strain to eliminate the possibility of bridging effects with endogenous Rif1, which we showed can form tetramers through a C-terminal domain (Shi et al., 2013). The Dbf4 interaction we detect is thus not mediated through other parts of Rif1. We next asked if Rif1-Glc7 affects phosphorylation of Dbf4 by monitoring cells released from G1 arrest into a synchronous S phase. We observed a prominent mobility shift of Dbf4-FLAG throughout S phase but no effect of Rif1 on this modification (Figure S3F).

Rif1 RVxF and SILK Mutations Affect Glc7 Recruitment and Replication Timing at Telomeres

Because Rif1 is concentrated at telomeres in yeast (Mishra and Shore, 1999) and known to play a role in determining their late replication (Lian et al., 2011), we next asked whether Rif1 recruits Glc7 to telomeres. Indeed, we detected modest but reproducible association of Glc7-Myc to both the chromosome VI-R and XV-L telomeres, at sequences very close to their linked ARS sites (Figure 4A). Significantly, this binding was reduced or eliminated by mutations in the RVxF and SILK motifs, to an extent similar to that observed in *rif1-ΔN* or *rif1Δ* mutants (Figure 4A). The effect of the RVxF and SILK mutations is not due to decreased recruitment of Rif1 to the telomeres (Figure S4). These data thus indicate that Glc7 interacts specifically with two telomeres in a manner that depends upon the Rif1 RVxF/SILK motifs.

We then asked whether reduced Glc7 binding caused by *rif1* mutations is associated with altered replication profiles at chromosome VI-R and XV-L telomeres. We measured replication kinetics in synchronized cells by performing chromatin immunoprecipitation (ChIP) on a Myc epitope-tagged Pol2 (DNA polymerase ε) protein (Bianchi and Shore, 2007). This analysis showed that, although the firing of the early *ARS607* occurs at the same time in wild-type and all *rif1* mutant cells, the appearance of Pol2 immediately adjacent to the VI-R and XV-L telomeres occurs approximately 15 min earlier in the *rif1* mutants, consistent with the activation of the telomere-proximal *ARS610* and *ARS1503* origins (Figures 4B, right panels, and S4B). We confirmed the earlier telomere replication in *rif1* mutants by measuring DNA amounts for the input samples of the Pol2 ChIP experiment (Figure 4B, left panels), normalized to the *ARS607* region, where replication timing is unaffected by Rif1 (Figure 4B, top right panel). The two telomeric regions that replicate after *ARS607* display a decrease in DNA copy number at the time of *ARS607* replication that is reversed when they themselves replicate (Figure 4B, left panels; compare 60 and 105 min time points). Consistent with the Pol2-Myc ChIP results, we observed an earlier copy-number increase at both telomeres in all the *rif1* mutants compared to wild-type (Figure 4B, left panels; see 75 and 90 min time points). Our results thus suggest that the Rif1-Glc7 interaction controls origin firing adjacent to two different telomeres.

DISCUSSION

The genetic analysis described here provides several insights into the role of Rif1 protein in the control of DNA replication in budding yeast by both genetically and physically linking its action to the PP1 phosphatase, Glc7, and by pinpointing its effect to specific events involved in pre-RC activation.

In considering how Rif1 might exert a negative effect on replication initiation, we focused on two short motifs (similar to RVxF/SILK) that were recently observed in fungal Rif1 N termini (Sreesankar et al., 2012) and that have previously been shown to be docking elements allowing regulatory proteins to bind to the conserved PP1 phosphatase (Cannon, 2010; Hendrickx et al., 2009). Our genetic data strongly suggest that these two motifs are together absolutely required for the ability of Rif1 to negatively regulate origin firing, because their mutation suppresses

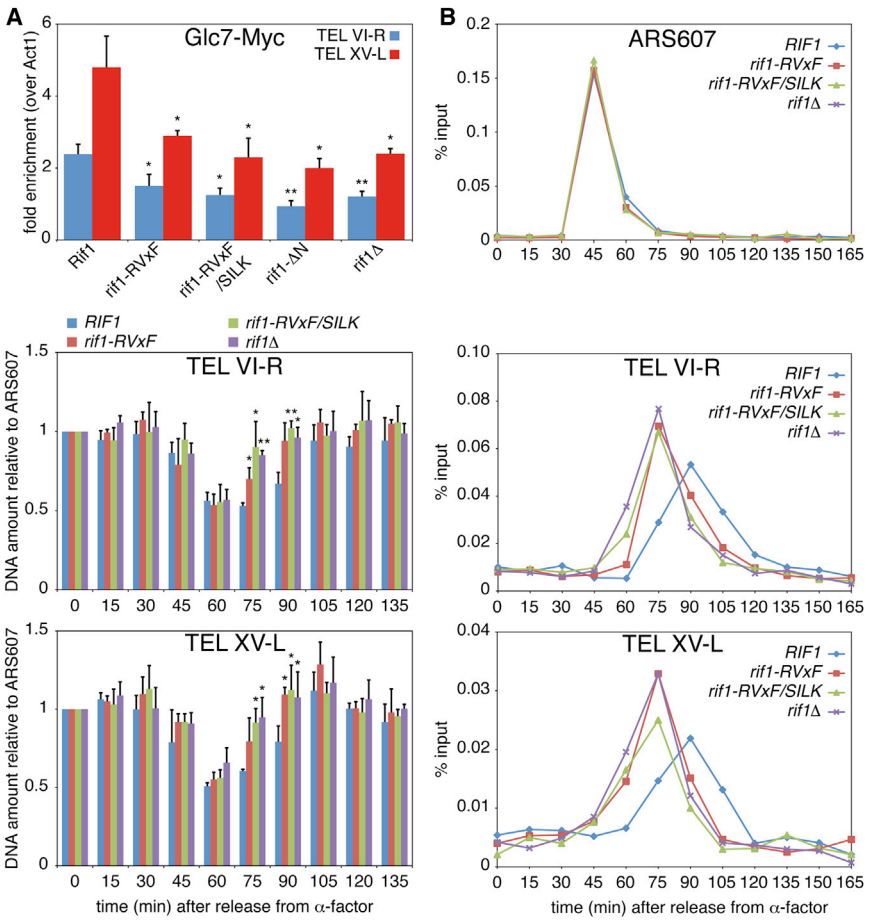

Figure 4. Telomeric Recruitment of Glc7 and Replication Timing Are Dependent upon Rif1 RVxF/SILK Motifs

(A) ChIP analysis of Glc7-Myc protein at the native chromosome VI-R and XV-L telomeres in *RIF1*, *rif1Δ*, and the indicated *rif1* deletion and point mutants cells. Results are reported as average fold enrichment and SD relative to the *ACT1* gene. Reduced recruitment of Glc7 is statistically significant in all of the *rif1* mutants tested (for TEL VI-R and TEL XV-L, respectively: *rif1-RVxF*, p = 0.049 and p = 0.048; *rif1-RVxF/SILK*, p = 0.007 and p = 0.038; *rif1-ΔN*, p = 0.004 and p = 0.037; *rif1Δ* p = 0.0013 and p = 0.019).

(B) *RIF1*, *rif1-RVxF*, and *rif1-RVxF/SILK* cells were blocked in G1 phase and then released at 18°C. Pol2-Myc protein recruitment was assayed by quantitative PCR-ChIP analysis on aliquots taken at the indicated times following release, using probe pairs near *ARS610* (adjacent to the chromosome VI-R telomere; position 270 kb), near *ARS607* (position 200 kb), and near *ARS1503* (adjacent to the chromosome XV-L telomere; left panels). DNA amounts in the input samples for Pol2-Myc ChIP, normalized to *ARS607* levels at t = 0, at the indicated time points following release from the G1 block. Results are reported as average and SD of three or four independent experiments (TEL VI-R: *rif1-RVxF* 75 min p = 0.03772; *rif1-RVxF/SILK* 75 min p = 0.01628, 90 min p = 0.01684; *rif1Δ* 75 min p = 0.00049, 90 min p = 0.04867. TEL XV-L: *rif1-RVxF* 75 min p = 0.00951; *rif1-RVxF/SILK* 75 min p = 0.01684, 90 min p = 0.04186; *rif1Δ* 75 min p = 0.02524, 90 min p = 0.04905; right panels).

See also Figure S4.

various ts-lethal mutations affecting pre-RC activation to nearly the same extent as deletion of the whole Rif1 open reading frame without having any obvious effect on Rif1 protein levels. Our observation that Rif1 coimmunoprecipitated with Glc7 in an RVxF/SILK-dependent manner further supports the idea that Rif1 and Glc7 indeed interact in G1 phase to affect replication. We note that a high-throughput proteomic screen of yeast kinases and phosphatases has also revealed a Rif1-Glc7 interaction (Breitkreutz et al., 2010).

Our detailed suppressor analysis of several different mutants involved in either pre-RC assembly or activation gives insights into the mode of Rif1-Glc7 action. We found no evidence for Rif1 action during pre-RC assembly but instead observed strong suppression by *rif1Δ* or *rif1-RVxF/SILK* mutations of specific alleles affecting pre-RC activation. Examination of the phosphorylation state of four different proteins involved in pre-RC activation provided further insights. Thus, we were able to show that Rif1 affects the phosphorylation state of both Mcm4 and Sld3 in a Cdc7 (DDK)-dependent manner in G1 cells, but not that of either Dbf4 or Sld2. Our phosphorylation data are thus strikingly consistent with the genetic suppression data, both of which point to the DDK axis of pre-RC activation and two DDK targets, Mcm4 and Sld3. Significantly, the S phase CDK target Sld2 is unaffected by Rif1 in either genetic or biochemical assays. Taking all of the above into account, we propose that Rif1-Glc7 inhibits replication initiation by counteracting the DDK in G1-phase cells. Our data are consistent with recent findings that Cdc45 and Sld3 (but not Sld2) are recruited to the pre-RC in G1 in a Cdc7-dependent manner and specifically at early-firing origins (Heller et al., 2011; Tanaka et al., 2011).

Although the suppression effect we observe for the *rif1-RVxF-SILK* mutation suggests that it might provoke a global increase in the phosphorylation state of at least two pre-RC activators, thus partially compensating for reduced DDK activity (*cdc7-4* or *dbf4-1*) or reduced activity of structural components (*sld3-4* and *dpb11-24*), it is still unclear if or how Rif1-Glc7 activity is targeted at a genome-wide level. Rif1 localizes to telomeres in budding yeast through an interaction with the telomere-binding protein Rap1 (Mishra and Shore, 1999; Shi et al., 2013) but has not been shown to bind elsewhere in the genome. Consistent with this, we do indeed find that telomeres are a direct site of Rif1-Glc7 action. One possibility is that the relief of Rif1-Glc7 inhibition at telomere-proximal origins in *rif1-RVxF-SILK* mutants is sufficient to cause the ts mutant rescue that we observe. However, we know that Rif1 mutants incapable of telomere localization, such as *rif1-ΔC* and *rif1-RBM* (Shi et al., 2013; data not shown), still strongly inhibit growth of *cdc7-4*, indicating that Rif1 does not have to be telomere-bound to counteract DDK function

globally. So, can Rif1-Glc7 exert their inhibitory effect at other specific genomic sites? Although we suspect that this is the case, we have so far failed to detect either Rif1 or Glc7 at nontelomeric origins by ChIP, so have no evidence that their effect at these sites is direct. Further work will be required to resolve this issue.

Our identification of Rif1 as a Dbf4-interacting protein in a yeast two-hybrid screen provides evidence for a physical link between Rif1 and the DDK. Interestingly, the C-terminal domain of Rif1 that suffices for this interaction is not required for Rif1 to exert a negative effect on pre-RC activity, and we detect no effect of Rif1 on Dbf4 phosphorylation. This argues that the DDK itself is not a direct target of Rif1-Glc7, nor is it required for Rif1-Glc7 to operate on its actual targets. Instead, the Dbf4-Rif1 interaction may be best understood as part of a feedback mechanism by which the DDK limits the inhibitory action of Rif1-Glc7 on the pre-RC during G1, up to the point at which early origins fire. Indeed, we note the presence of five phospho-serine residues flanking the RVxF/SILK motifs in Rif1 that have been identified in proteomic studies (http://www.phosphopep.org/) and which are potential DDK targets. We thus speculate that the DDK targets the Rif1 N terminus in order to limit Glc7 recruitment and action at origins to the G1 phase. This model is consistent with the proposal that DDK activity increases as cells move into and through S phase (Rhind et al., 2010) and is also supported by our biochemical data.

We note that the findings described here, and in two recent related reports (Davé et al., 2014; Hiraga et al., 2014), are likely to have important implications for Rif1 function in other eukaryotes, including mammals. Recent reports show that fission yeast (Hayano et al., 2012), mouse (Cornacchia et al., 2012), and human Rif1 (Yamazaki et al., 2012) homologs are also involved in regulation of the temporal program of DNA replication. Furthermore, mammalian RIF1 has been shown to interact with PP1 (Moorhead et al., 2008). We thus predict that a RIF1-PP1 interaction in mammalian cells (as well as in fission yeast) will play a role in controlling the replication timing program in these systems, presumably through similar targets in the pre-RC activation pathway, many of which are also highly conserved between yeast and human.

EXPERIMENTAL PROCEDURES

Strains and Plasmids

All yeast strains and plasmids used in this study are listed in Tables S1 and S2, respectively. General yeast manipulations were done according to standard methods (Rose et al., 1990).

Viability Assays

Yeast strains were grown in the appropriate media to a concentration of 1 × 10^7 cells/ml. Serial 10-fold dilutions were spotted on plates containing yeast extract, peptone, adenine, and dextrose medium (YPAD) or selective medium at the indicated temperature. Plates were photographed after 2 days of incubation.

Western Blotting and CoIP Assays

Protein extracts (trichloroacetic acid-urea method) and SDS-PAGE western blot analyses were performed as described (Lempiäinen et al., 2009). See Supplemental Experimental Procedures for further details. For coimmunoprecipitation experiments, 500 ml of cells in exponential growth were treated with 50 ng/ml of α factor (Bachem) for 120 min in YPAD at 30°C. Cells were harvested and lysed by bead beating (0.5 mm zirconia-silica beads) in a buffer containing 20 mM Tris (pH 8.0), 150 mM KCl, 1 mM EDTA, 1% NP-40, 20% glycerol, 1 mM dithiothreitol, and 1 mM phenylmethanesulfonylfluoride, supplemented with a protease and phosphatase inhibitor mix (Roche Molecular Biochemicals). Lysates precleared by centrifugation were subjected to anti-FLAG M2 or anti-Myc (9E10) immunoprecipitation by following the manufacturer's instructions (Sigma Aldrich). The beads were washed three times with the lysis buffer, and the immunoprecipitates were eluted in SDS sample buffer.

Yeast Two-Hybrid Screens and Assays

Yeast two-hybrid screens and quantitative beta-galactosidase assays were carried out as described previously (James et al., 1996).

ChIP and DNA Quantification Assays

ChIP assays were performed as described previously (Bianchi et al., 2004), with minor modifications (see Supplemental Experimental Procedures for details and for description of the DNA quantification assay).

Cell Synchrony Experiments

Overnight cultures of *MATa bar1Δ* strains were diluted 10-fold into 450 ml of YPAD. After 3.5 hr growth at 30°C, cultures were blocked by treatment with 50 ng/ml of α factor (Bachem) for 130 min in YPAD at 30°C. Cells were released from the arrest by washing and by Pronase Nuclease-free treatment (Calbiochem; 50 mg total) and then placed in YPAD medium at 18°C. Samples were taken at 15 min intervals for ChIP and FACS analysis. Cell-cycle synchrony and release were checked by microscope and FACS analysis as described previously (Bianchi and Shore, 2007).

Statistical Analysis

The differences in values obtained in either ChIP or DNA quantification assays were assessed for significance with Student's t test. Average values and SD are reported.

SUPPLEMENTAL INFORMATION

Supplemental Information includes Supplemental Experimental Procedures, four figures, and two tables and can be found with this article online at http://dx.doi.org/10.1016/j.celrep.2014.03.010.

ACKNOWLEDGMENTS

We thank I. Marcomini for help in initiating the project; N. Roggli for expert artwork; H. Araki, J. Diffley, S. Yerlikaya, R. Loewith, P. James, and E. Craig for providing strains and plasmid libraries; and A. Bianchi and C. Cooley for advice on Cdc7 inactivation protocols. These studies were supported by grants from the Swiss National Fund to D.S. and N.H.T. D.S. also acknowledges financial support from the Republic and Canton of Geneva.

Received: January 15, 2014
Revised: February 15, 2014
Accepted: March 6, 2014
Published: March 27, 2014

REFERENCES

Aparicio, O.M. (2013). Location, location, location: it's all in the timing for replication origins. Genes Dev. *27*, 117–128.

Araki, H. (2011). Initiation of chromosomal DNA replication in eukaryotic cells; contribution of yeast genetics to the elucidation. Genes Genet. Syst. *86*, 141–149.

Bianchi, A., and Shore, D. (2007). Early replication of short telomeres in budding yeast. Cell *128*, 1051–1062.

Bianchi, A., Negrini, S., and Shore, D. (2004). Delivery of yeast telomerase to a DNA break depends on the recruitment functions of Cdc13 and Est1. Mol. Cell *16*, 139–146.

Breitkreutz, A., Choi, H., Sharom, J.R., Boucher, L., Neduva, V., Larsen, B., Lin, Z.Y., Breitkreutz, B.J., Stark, C., Liu, G., et al. (2010). A global protein kinase and phosphatase interaction network in yeast. Science *328*, 1043–1046.

Cannon, J.F. (2010). Function of protein phosphatase-1, Glc7, in Saccharomyces cerevisiae. Adv. Appl. Microbiol. *73*, 27–59.

Chen, S., and Bell, S.P. (2011). CDK prevents Mcm2-7 helicase loading by inhibiting Cdt1 interaction with Orc6. Genes Dev. *25*, 363–372.

Cornacchia, D., Dileep, V., Quivy, J.P., Foti, R., Tili, F., Santarella-Mellwig, R., Antony, C., Almouzni, G., Gilbert, D.M., and Buonomo, S.B. (2012). Mouse Rif1 is a key regulator of the replication-timing programme in mammalian cells. EMBO J. *31*, 3678–3690.

Cosgrove, A.J., Nieduszynski, C.A., and Donaldson, A.D. (2002). Ku complex controls the replication time of DNA in telomere regions. Genes Dev. *16*, 2485–2490.

Davé, A., Cooley, C., Garg, M., and Bianchi, A. (2014). Protein phosphatase 1 recruitment by Rif1 regulates DNA replication origin firing by counteracting DDK activity. Cell Rep. Published online April 10, 2014. http://dx.doi.org/10.1016/j.celrep.2014.02.019.

Donaldson, A.D. (2005). Shaping time: chromatin structure and the DNA replication programme. Trends Genet. *21*, 444–449.

Hardy, C.F.J., Sussel, L., and Shore, D. (1992). A RAP1-interacting protein involved in transcriptional silencing and telomere length regulation. Genes Dev. *6*, 801–814.

Hayano, M., Kanoh, Y., Matsumoto, S., Renard-Guillet, C., Shirahige, K., and Masai, H. (2012). Rif1 is a global regulator of timing of replication origin firing in fission yeast. Genes Dev. *26*, 137–150.

Heller, R.C., Kang, S., Lam, W.M., Chen, S., Chan, C.S., and Bell, S.P. (2011). Eukaryotic origin-dependent DNA replication in vitro reveals sequential action of DDK and S-CDK kinases. Cell *146*, 80–91.

Hendrickx, A., Beullens, M., Ceulemans, H., Den Abt, T., Van Eynde, A., Nicolaescu, E., Lesage, B., and Bollen, M. (2009). Docking motif-guided mapping of the interactome of protein phosphatase-1. Chem. Biol. *16*, 365–371.

Hiraga, S., Alvino, G.M., Chang, F., Lian, H.Y., Sridhar, A., Kubota, T., Brewer, B.J., Weinreich, M., Raghuraman, M.K., and Donaldson, A.D. (2014). Rif1 controls DNA replication by directing protein phosphatase 1 to reverse Cdc7-mediated phosphorylation of the MCM complex. Genes Dev. *28*, 372–383.

James, P., Halladay, J., and Craig, E.A. (1996). Genomic libraries and a host strain designed for highly efficient two-hybrid selection in yeast. Genetics *144*, 1425–1436.

Labib, K. (2010). How do Cdc7 and cyclin-dependent kinases trigger the initiation of chromosome replication in eukaryotic cells? Genes Dev. *24*, 1208–1219.

Lempiäinen, H., Uotila, A., Urban, J., Dohnal, I., Ammerer, G., Loewith, R., and Shore, D. (2009). Sfp1 interaction with TORC1 and Mrs6 reveals feedback regulation on TOR signaling. Mol. Cell *33*, 704–716.

Lian, H.Y., Robertson, E.D., Hiraga, S., Alvino, G.M., Collingwood, D., McCune, H.J., Sridhar, A., Brewer, B.J., Raghuraman, M.K., and Donaldson, A.D. (2011). The effect of Ku on telomere replication time is mediated by telomere length but is independent of histone tail acetylation. Mol. Biol. Cell *22*, 1753–1765.

Lopez-Mosqueda, J., Maas, N.L., Jonsson, Z.O., Defazio-Eli, L.G., Wohlschlegel, J., and Toczyski, D.P. (2010). Damage-induced phosphorylation of Sld3 is important to block late origin firing. Nature *467*, 479–483.

Mantiero, D., Mackenzie, A., Donaldson, A., and Zegerman, P. (2011). Limiting replication initiation factors execute the temporal programme of origin firing in budding yeast. EMBO J. *30*, 4805–4814.

Mishra, K., and Shore, D. (1999). Yeast Ku protein plays a direct role in telomeric silencing and counteracts inhibition by rif proteins. Curr. Biol. *9*, 1123–1126.

Moorhead, G.B., Trinkle-Mulcahy, L., Nimick, M., De Wever, V., Campbell, D.G., Gourlay, R., Lam, Y.W., and Lamond, A.I. (2008). Displacement affinity chromatography of protein phosphatase one (PP1) complexes. BMC Biochem. *9*, 28.

Rhind, N., Yang, S.C., and Bechhoefer, J. (2010). Reconciling stochastic origin firing with defined replication timing. Chromosome Res. *18*, 35–43.

Rose, M.D., Winston, F., and Hieter, P. (1990). Methods in Yeast Genetics: A Laboratory Course Manual (Plainview, New York: Cold Spring Harbor Press).

Sheu, Y.J., and Stillman, B. (2006). Cdc7-Dbf4 phosphorylates MCM proteins via a docking site-mediated mechanism to promote S phase progression. Mol. Cell *24*, 101–113.

Shi, T., Bunker, R.D., Mattarocci, S., Ribeyre, C., Faty, M., Gut, H., Scrima, A., Rass, U., Rubin, S.M., Shore, D., and Thomä, N.H. (2013). Rif1 and Rif2 shape telomere function and architecture through multivalent Rap1 interactions. Cell *153*, 1340–1353.

Siddiqui, K., On, K.F., and Diffley, J.F. (2013). Regulating DNA replication in eukarya. Cold Spring Harb. Perspect. Biol. *5*, pii: a012930.

Sreesankar, E., Senthilkumar, R., Bharathi, V., Mishra, R.K., and Mishra, K. (2012). Functional diversification of yeast telomere associated protein, Rif1, in higher eukaryotes. BMC Genomics *13*, 255.

Stevenson, J.B., and Gottschling, D.E. (1999). Telomeric chromatin modulates replication timing near chromosome ends. Genes Dev. *13*, 146–151.

Tanaka, S., Umemori, T., Hirai, K., Muramatsu, S., Kamimura, Y., and Araki, H. (2007). CDK-dependent phosphorylation of Sld2 and Sld3 initiates DNA replication in budding yeast. Nature *445*, 328–332.

Tanaka, S., Nakato, R., Katou, Y., Shirahige, K., and Araki, H. (2011). Origin association of Sld3, Sld7, and Cdc45 proteins is a key step for determination of origin-firing timing. Curr. Biol. *21*, 2055–2063.

Yamazaki, S., Ishii, A., Kanoh, Y., Oda, M., Nishito, Y., and Masai, H. (2012). Rif1 regulates the replication timing domains on the human genome. EMBO J. *31*, 3667–3677.

Zegerman, P., and Diffley, J.F. (2007). Phosphorylation of Sld2 and Sld3 by cyclin-dependent kinases promotes DNA replication in budding yeast. Nature *445*, 281–285.

Zegerman, P., and Diffley, J.F. (2010). Checkpoint-dependent inhibition of DNA replication initiation by Sld3 and Dbf4 phosphorylation. Nature *467*, 474–478.

Supplemental Information for:

Rif1 controls DNA replication timing in yeast through the PP1 phosphatase Glc7

Stefano Mattarocci[1*], Maksym Shyian[1*], Laure Lemmens[1], Pascal Damay[1], Dogus Murat Altintas[1], Tianlai Shi[2, 4], Clinton R. Bartholomew[3], Nicolas Thomä[2], Christopher F. J. Hardy[3], and David Shore[1, 5]

[1]Department of Molecular Biology and Institute of Genetics and Genomics of Geneva (iGE3), University of Geneva, 30 quai Ernest-Ansermet, Geneva 4, CH-1211 Switzerland.

[2]Friedrich Miescher Institute for Biomedical Research, Maulbeerstrasse 66, CH-4058 Basel, Switzerland.

[3]Department of Cell and Developmental Biology, Vanderbilt University Medical Center, T-2212 Medical Center North, Nashville, TN 37232-2175, USA.

[4]current address: Hoffmann-La Roche Ltd, Basel, Switzerland

*These authors contributed equally to this work

[5]Corresponding author: David.Shore@unige.ch

Experimental Procedures

Site-specific *in vivo* mutagenesis

Mutations in SVAF (V116R-F118R) and SILR (I147R-L148R-R149A) motifs of Rif1 and deletion of the N-terminal region of Rif1 (from residues 2 to 176) were generated by the “delitto perfetto” method (Stuckey et al., 2011). Briefly, a COunterselectable REporter (CORE) cassette, containing Uracil and KAN markers, is inserted at the locus to be altered. Then appropriate targeting oligonucleotides are transformed into the cells recombining in this locus such that the CORE cassette is lost and the desired change is generated.

Western blot analysis

Nine ml of cells grown in YPAD medium were treated with 600 µl of TCA 100% and kept on ice for 10 minutes. After two washes in acetone (100%), the pellets were dried and resuspended in 100 µl of Urea buffer (50 mM Tris-Cl pH 7.5, 5 mM EDTA, 6 M Urea, 1% SDS), then lysed using 0.5 mm glass beads in a Bead Beater. The protein extracts were resuspended in 200 µl in 1X Laemmli sample buffer (80 mM TrisCl pH6.8, 2% SDS, 10% Glycerol, 0.01% BromoPhenol Blue, 100 mM DTT) and boiled at 95°C for 5 minutes. The samples were then separated on an SDS-PAGE gel and western blotting was performed (antibodies used: Anti-Myc (Cell Signaling, 9B11 mAb #2276, dilution 1:10000), anti-FLAG (Sigma, anti-Flag M2 mAb F3165, dilution 1:7500), anti-Actin (Abcam, ab 8224, dilution 1:10000), anti-Clb2 (Santa Cruz Biotech, sc-9071, dilution 1:100). Secondary antibodies: horseradish peroxidase-conjugated donkey anti-mouse or anti-rabbit antibody (Promega, dilution: 1:10000)). For the phos-tag gels, total protein extracts were prepared using the TCA-Urea method. Equal volumes of protein extract samples were resolved in parallel on standard degased 6% SDS-polyacrylamide gels and 6% gels supplemented with 50 µM Phos-tag ligand (AAL-107; NARD Institute, Amagasaki, Japan) and 100 µM $MnCl_2$, according to (Kinoshita et al., 2006). The Phos-tag containing gels were washed two times with western blot transfer buffer supplemented with 1 mM EDTA and once with transfer buffer without EDTA. The proteins were

transferred to a nitrocellulose membrane, probed with the respective antibodies and detected with ECL (GE Healthcare Life Sciences).

Analysis of Mcm4 and Sld3 phosphorylation

Cells were grown for 3 hours on YPAD medium at 25°C or 30°C (for, respectively, *cdc7-4* and *CDC7* cells) until exponential phase. *Bar1Δ* cells were shifted to 37°C in pre-warmed YPAD medium in the presence of α-factor (500 ng/ml; Bachem) for 2 hours. *BAR1* cells were shifted to 37°C in pre-warmed YPAD medium in the presence of α-factor 5 µg/ml for 1 hour, then pelleted and resuspended in fresh pre-warmed medium with 5 µg/ml of α-factor and incubated for 1 hour at 37°C. Cells were then collected for protein extraction.

ChIP assay

Cells were cross-linked in 1% formaldehyde, lysed by bead-beating (0.5mm Zirconia-Silica beads) and then sonicated using a Bioruptor (Diagenode) device (10 cycles of 30 s sonication followed by a 60 s pause). Antibodies against the Myc epitope (9E10 from culture supernatant) were used for immunoprecipitation of Myc-tagged proteins (Pol2 and Glc7). Immunoprecipitation of RPA was performed with an anti-RPA antibody (Pierce Biotechnology, scRPA PA1-10301). Dynabeads M280 coupled to sheep anti-mouse or anti-rabbit IgG (Dynal) were used for anti-Myc and anti-RPA antibodies, respectively.

We quantified immunoprecipitated DNA by real-time PCR on a LightCycler 480 (Roche) using 2X SYBR green I Master Mix (Roche). Enrichment of amplicons SBR11 and SBR25 (located 300 bp from the ends of chromosomes XV-L and VI-R, respectively) over an internal control (*ACT1*) was determined after normalization with values obtained for input samples. For synchronization experiments measuring DNA polymerase ε (Pol2-Myc) and RPA localization, percent of input for amplicons located 300 bp from *ARS607,* from *ARS1412*, and from the ends of chromosomes XV-L and VI-R, was determined. For each

protein, results were obtained from three or more independent biological replicates. For ChIP experiments in synchronized cells (Pol2-Myc and RPA) representative data are shown for single experiments. For ChIP experiments in unsynchronized cells (Glc7-Myc) data are reported as average fold enrichment (bars) for 3 or more experiments, with standard deviations indicated by lines above.

DNA quantification

Forty ml of culture were crosslinked with 1% of formaldehyde. After formaldehyde-quenching with 2 ml of 2.5M of glycine, cells were washed two times in HBS buffer (50 mM HEPES pH 7.5, 140 mM NaCl) then the pellets were re-suspended in 600ul of lysis buffer (50 mM HEPES pH 7.5, 140 mM NaCl, 1 mM EDTA pH 8.0, 1% IGEPAL CA-630, 2.4 mM sodium deoxycholate) and lysed using 0.5 mm zirconia silica beads in a Bead Beater. After sonication using a Bioruptor (Diagenode) (10 cycles of 30 seconds sonication followed by a 60 seconds pause), extracts were pelleted and 10 µl of supernatant was de-crosslinked at 65°C in 120 µl of lysis buffer. DNA was purified using an AccuPrep PCR purification kit (Bioneer) and qPCR was performed as described above (see ChIP assay description).

FACS analysis

After fixation in 70% ethanol and treatment for 3 hours with 200 µg/ml RNAse, cells were stained with 10 µg/ml Propidium Iodide (PI) and then analyzed as described previously (Bianchi & Shore, 2007).

Supplementary Figure Legends

Figure S1. Related to Figure 1. The protein levels of pre-RC activators are unaffected by *rif1*Δ.

SDS-PAGE western blot using anti-Myc or anti-FLAG antibodies of extracts from either *RIF1* (WT) or *rif1*Δ cells expressing Sld3-13xMyc, Cdc45-13xMyc, Dpb11-13xMyc, Dbf4-FLAG or Sld2-FLAG from their endogenous loci. As a negative control for the anti-Myc blot, *RIF1* or *rif1*Δ untagged strains were examined. The blots were also probed with anti-Actin antibody as a loading control.

Figure S2. Related to Figure 2. Mutations in Rif1 RVxF and SILK motifs suppress *cdc45-27* growth defects and do not affect Rif1 protein stability.

(A) Cells with the indicated genotypes were grown and spotted on YPAD plates as indicated in Figure 1.

(B) SDS-PAGE western blot using anti-Myc or anti-Actin antibodies of extracts from cells expressing either Rif1-Myc, rif1-RVxF-Myc, rif1-SILK-Myc, rif1-RVxF/SILK-Myc or rif1-ΔN-Myc (ΔN, deletion of residues 2 to 176).

Figure S3. Related to Figure 3. Rif1 interacts with Glc7 and regulates the phosphorylation level of Mcm4 and Sld3 proteins.

(A) Western blot using anti-Myc mAb, following immunoprecipitation with anti-FLAG M2 beads from cells expressing Glc7-FLAG and Rif1-Myc, or from control cells expressing only Rif1-Myc. Extracts were prepared from G1-arrested cells. The same samples were analyzed by western blot using anti-FLAG antibody (left panel). Western blot using anti-FLAG, following immunoprecipitation with anti-Myc antibody from G1-arrested cells expressing Glc7-Myc and Rif1-FLAG, or from control cells expressing only Rif1-FLAG. The same samples were analyzed by western blot using anti-Myc antibody (middle panel). Western blot using anti-Myc mAb, following immunoprecipitation with anti-FLAG M2 beads from G1-

arrested cells expressing Glc7-FLAG and either Rif1-Myc (WT) or Rif1-RVxF-SILK-Myc (mut). The same samples were analyzed by western blot using anti-FLAG antibody (right panel).

(B) FACS and SDS-PAGE western blot analysis of *RIF1* or *rif1*Δ cells arrested in G1 phase and released into a synchronous S phase at 18°C. Aliquots were taken at the indicated time points. Western blots were probed with anti-Clb2 (a G2/M phase cyclin) or anti-Actin antibodies. As, Asynchronous culture (left panels). RPA protein recruitment was assayed by qPCR-ChIP analysis on aliquots taken (either from *RIF1* or *rif1*Δ cells) at the indicated times following release, using probe pairs near the early *ARS607* origin or near the late *ARS1412* origin (right panel).

(C) *RIF1 and rif1*Δ (left panel) or *RIF1 and rif1-RVxF/SILK* (right panel) cells, all expressing Mcm4-Myc, were arrested in G1 phase and then released into a synchronous S phase. Extracts from aliquots taken at the indicated times following release were loaded on a single SDS-PAGE gel. Western blots were probed with anti-Myc or anti-Actin antibodies.

(D) Phos-tag SDS-PAGE western blot using anti-Myc antibody of extracts from either *RIF1* or *rif1*Δ cells expressing Sld3-Myc from the endogenous *SLD3* locus. Cells were G1-arrested and released into a synchronous S phase and aliquots were taken at the indicated time points. The same samples were also analyzed by SDS-PAGE western blot to measure the total level of Sld3 protein (left panel). *CDC7* or *cdc7-4* cells expressing Sld3-Myc were grown at 25°C and then shifted to the indicated temperatures in the presence of α-factor for 2 hours. Western blots were carried out as above (right panel).

(E) Phos-tag SDS-PAGE and normal SDS-PAGE western blots using anti-Myc antibody from extracts of *RIF1* or *rif1*Δ cells (expressing Orc6-Myc from the endogenous *ORC6* locus) arrested in G1 or G2 phase by α-factor or nocodazole (10 μg/ml) treatments, respectively.

(F) *RIF1* and *rif1*Δ cells, all of which express a Dbf4-FLAG protein from the endogenous *DBF4* locus, were G1-arrested and released into a synchronous S phase. Aliquots were taken at the indicated time points and protein extracts were prepared and analyzed by Phos-TAG or standard SDS-PAGE western blot using anti-FLAG mAb (*, non-specific band).

Figure S4. Related to Figure 4. Mutations in Rif1 RVxF and SILK motifs affect telomere replication timing, but not the recruitment of Rif1 at telomeres.

(A) Recruitment of Rif1 protein at the native telomeres on chromosomes VI-R and XV-L in *RIF1, rif1-RVxF, rif1-SILK* and *rif1-RVxF/SILK* cells. Results are reported as average fold-enrichment and standard deviation, relative to the *ACT1* gene.

(B) DNA polymerase ε (Pol2-Myc) protein recruitment was assayed by qPCR-ChIP analysis (using probe pairs near *ARS610* and *ARS1503*, which are adjacent to the chromosome VI-R and XV-L telomeres, respectively) from cells expressing either wild-type Rif1, rif1-RVxF or rif1-RVxF/SILK mutant proteins, at the indicated times following release from α-factor arrest. Two independent experiments are shown for each telomere.

Table S1. Genotypes of yeast strains used in this study.

Strain Name	Relevant genotype	Figure	Source
W303-1A	*MAT***a** *leu2-3,112 trp1-1 can1-100 ura3-1 ade2-1 his3-11,15*		
YMS331	W303-1A *rif1::NatMX4*	1, 2, S2	this study
YKB2	W303-1A *cdc7-4*	1A, 2	(Bousset and Diffley, 1998)
YYK14	W303-1A *sld3-4 bar1Δ::hisG*	1A, 2B	(Tanaka et al., 2011)
YNIG63	W303-1A *dpb11-24 bar1Δ::hisG*	1A, S2A	(Tanaka et al., 2007)
YCH265	W303-1A *dbf4-1*	1A, S2A	(Cheng et al., 1999)
YYK32	W303-1A *cdc45-27 bar1Δ::hisG*	1A, S2A	(Kamimura et al., 2001)
YCH178	W303-1B *MAT*α *orc5-1*	1B	(Loo et al., 1995)
YCH175	W303-1B *cdc6-1*	1B	(Liang and Stillman, 1997)
YCH174	W303-1A *cdc46-1*	1B	(Li and Herskowitz, 1993)
YSM291-1	W303-1a *cdc7-4 rif1::NatMX4*	1A, 2	this study
YIM4	W303-1A *sld3-4 rif1::NatMX4*	1A, 2B	this study
YSM247	W303-1A *dpb11-24 rif1::NatMX4*	1A, S2A	this study
YCH4248	W303-1A *dbf4-1 rif1::TRP1*	1A, S2A	this study
YSM246	W303-1A *cdc45-27 rif1::NatMX4*	1A, S2A	this study
YCH4161	W303-1B *orc5-1 rif1::KANMX4*	1B	this study
YSM276	W303-1B *cdc6-1 rif1::NatMX4*	1B	this study
YCH4178	W303-1B *cdc46-1 rif1::KanMX4*	1B	this study
YYK7	*sld2-6 ade2-1 bar1Δ::URA3 can1-100 his3-11,15 leu2-3,112 sld2::LEU2 trp1-1 ura3-1* [YCp22-sld2-6]	3E	(Tanaka et al., 2011)
YSM336	*sld2-6 rif1::NatMX4*	3E	this study
YSM264	W303-1A *cdc7-4 rif1Δ2-176-13MYC::HIS3MX6*	2A, 2B	this study
YSM283	W303-1A *cdc7-4 rif1Δ1323-1916-13MYC::HIS3MX6*	2A	this study
YSM130-1	W303-1A *cdc7-4 rif1-V116R-F118R*	2B	this study
YSM188	W303-1A *cdc7-4 rif1-I147R-L148R-R149A*	2B	this study
YSM189	W303-1A *cdc7-4 rif1-V116R-F118R-I147R-L148R-R149A*	2B	this study
YSM187	W303-1A *sld3-4 rif1-V116R-F118R*	2B	this study
YSM323	W303-1A *sld3-4 rif1-V116R-F118R-I147R-L148R-R149A*	2B	this study
YSM198	W303-1A *dpb11-24 rif1-V116R-F118R*	2B	this study
YSM324	W303-1A *dbf4-1 rif1-V116R-F118R-I147R-L148R-R149A*	2B	this study
YSM197	W303-1A *cdc45-27 rif1-V116R-F118R*	S2A	this study
YSM315	W303-1A *cdc7-4* pRS426	2D	this study
YSM316	W303-1A cdc7-4 pRS426-PGLC7-GLC7	2D	this study
YSM317	W303-1A *cdc7-4 rif1::NatMX4* pRS426	2D	this study
YSM318	W303-1A *cdc7-4 rif1::NatMX4* pRS426-PGLC7-GLC7	2D	this study
YSM313	W303-1A *bar1Δ* pRS426	2D	this study

YSM314	W303-1A *bar1Δ* pRS426-PGLC7-GLC7	2D	this study
YLL359	W303-1A *bar1Δ CDC45-13MYC::HIS3MX6*	S1	this study
YLL382	W303-1A *bar1Δ DPB11-13MYC::HIS3MX6*	S1	this study
YLL377	W303-1A *bar1Δ DBF4-FLAG::KanMX3*	3F, S1, S3F	this study
YLL384	W303-1A *bar1Δ SLD2-FLAG::HphMX3*	S1	this study
YLL368	W303-1A *bar1Δ CDC45-13MYC::HIS3MX6 rif1::NatMX4*	S1	this study
YLL383	W303-1A *bar1Δ DPB11-13MYC::HIS3MX6 rif1::NatMX4*	S1	this study
YLL378	W303-1A *bar1Δ DBF4-FLAG::KanMX3 rif1::NatMX4*	3F, S1, S3F	this study
YLL385	W303-1A *bar1Δ SLD2-FLAG::HphMX3 rif1::NatMX4*	S1	this study
YSM20-2	W303-1A *bar1Δ RIF1-13MYC::HIS3MX6*	3A	this study
YSM280-1	W303-1A *bar1Δ RIF1-13MYC::HIS3MX6 GLC7-FLAG::KanMX3*	3A	this study
YSM266	W303-1A *bar1Δ MCM4-13MYC::HIS3MX6*	3B, 3C, S3C	this study
YSM269	W303-1A *bar1Δ MCM4-13MYC::HIS3MX6 rif1::NatMX4*	3B, 3C, S3C	this study
YSM298	W303-1A *bar1Δ MCM4-13MYC::HIS3MX6 rif1-V116R-F118R-I147R-L148R-R149A*	3B, 3C, S3B	this study
YSM299	W303-1A *cdc7-4 MCM4-13MYC::HIS3MX6*	3B	this study
YSM319	W303-1A *cdc7-4 MCM4-13MYC::HIS3MX6 rif1::NatMX4*	3B	this study
YMS419	W303-1A *bar1Δ SLD3-13MYC::HIS3MX6*	3D, S1, S3D	this study
YMS438	W303-1A *bar1Δ SLD3-13MYC::HIS3MX6 rif1::NatMX4*	3D, S1, S3D	this study
YMS497	W303-1A *cdc7-4 SLD3-13MYC::HIS3MX6 rif1::NatMX4*	3D	this study
YMS488	W303-1A *bar1Δ SLD3-13MYC::HIS3MX6 sml1::HphMX4*	3D	this study
YMS489	W303-1A *bar1Δ SLD3-13MYC::HIS3MX6 sml1::HphMX rif1::NatMX4*	3D	this study
YMS493	W303-1a *bar1Δ SLD3-13MYC::HIS3MX6 sml1::HphMX mec1::KanMX6*	3D	this study
YMS494	W303-1a *bar1Δ SLD3-13MYC::HIS3MX6 sml1::HphMX mec1::KANMX6*	3D	this study
Y1162	PJ69-4 (*MAT***a** *trp1-901 leu2-3,112 ura3-52 his3-200 gal4Δ gal80Δ LYS2::GAL1-HIS3 GAL2-ADE2 met2::GAL7-lacZ*) *rif1::NatMX4*	3FE	this study
YMS442	W303-1A *bar1Δ ORC6-13MYC::HIS3MX6*	S3E	this study
YMS443	W303-1A *bar1Δ ORC6-13MYC::HIS3MX6 rif1::NatMX4*	S3E	this study
YMS456	W303-1A *GLC7-13MYC::HIS3MX6 RIF1-FLAG::KanMX3*	S3A	this study
YMS454	W303-1A *RIF1-FLAG::KANMX3*	S3A	this study
YSM223	W303-1A *GLC7-13MYC::HIS3MX6*	4A	this study
YSM224	W303-1A *rif1-V116R-F118R-I147R-L148R-R149A GLC7-13MYC::HIS3MX6*	4A	this study
YSM251	W303-1A *rif1Δ2-176 GLC7-13MYC::HIS3MX6*	4A	this study
YSM132-9	W303-1A *rif1::NatMX4 GLC7-13MYC::HIS3MX6*	4A	this study
YSM117-5	W303-1A *cdc7-4 RIF1-13MYC::HIS3MX6*	S4A	this study
YSM133	W303-1A *cdc7-4 rif1-V116R-F118R-13MYC::HIS3MX6*	S4A	this study

YSM248	W303-1A *cdc7-4 rif1-I147R-L148R-R149A-13MYC::HIS3MX6*	S4A	this study
YSM249	W303-1A *cdc7-4 rif1-V116R-F118R-I147R-L148R-R149A-13MYC::HIS3MX6*	S4A	this study
YLL237	W303-1A *RAD5+ bar1Δ FLAG-POL1 POL2-13MYC::KanMX3*	4B, S4B	this study
YLL433	W303-1A *RAD5+ bar1Δ FLAG-POL1 POL2-13MYC::KanMX3 rif1-V116R-F118R*	4B, S4B	this study
YSM312-1	W303-1A *RAD5+ bar1Δ POL2-13MYC::KANMX3 rif1-V116R-F118R-I147R-L148R-R149A*	4B, S4B	this study

Supplmentary Table S2. Plasmids used in this study.

Plasmid name	Vector::insert	Figure	Source
pSY64	pRS426::P_{GLC7}-GLC7	2D	R. Loewith lab
pCH960	pGBDU::DBF4	3E	this study
pCH1707	pGAD-C1::RIF1(1674-1916)	3E	this study
TL208	pGAD-C1::RIF1(1710-1916)	3E	Shi et al., 2013
TL233	pGAD-C1::RIF1(1710-1916 - I1760R)	3E	Shi et al., 2013
TL206	pGAD-C1::RIF1(1-1322)	3E	this study
TL225	pGBD-C1::RAP1(672-827)	3E	Shi et al., 2013

Supplemental references

Bousset, K., and Diffley, J.F. (1998). The Cdc7 protein kinase is required for origin firing during S phase. Genes Dev *12*, 480-490.

Cheng, L., Collyer, T., and Hardy, C.F. (1999). Cell cycle regulation of DNA replication initiator factor Dbf4p. Mol Cell Biol *19*, 4270-4278.

Kamimura, Y., Tak, Y.S., Sugino, A., and Araki, H. (2001). Sld3, which interacts with Cdc45 (Sld4), functions for chromosomal DNA replication in Saccharomyces cerevisiae. The EMBO journal *20*, 2097-2107.

Kinoshita, E., Kinoshita-Kikuta, E., Takiyama, K., and Koike, T. (2006). Phosphate-binding tag, a new tool to visualize phosphorylated proteins. Molecular & cellular proteomics : MCP *5*, 749-757.

Li, J.J., and Herskowitz, I. (1993). Isolation of *ORC6*, a component of the yeast origin recognition complex by a one-hybrid system. Science *262*, 1870-1874.

Liang, C., and Stillman, B. (1997). Persistent initiation of DNA replication and chromatin-bound MCM proteins during the cell cycle in cdc6 mutants. Genes Dev *11*, 3375-3386.

Loo, S., Fox, C.A., Rine, J., Kobayashi, R., Stillman, B., and Bell, S. (1995). The origin recognition complex in silencing, cell cycle progression, and DNA replication. Mol Biol Cell *6*, 741-756.

Stuckey, S., Mukherjee, K., and Storici, F. (2011). In vivo site-specific mutagenesis and gene collage using the delitto perfetto system in yeast Saccharomyces cerevisiae. Methods Mol Biol *745*, 173-191.

Tanaka, S., Nakato, R., Katou, Y., Shirahige, K., and Araki, H. (2011). Origin association of Sld3, Sld7, and Cdc45 proteins is a key step for determination of origin-firing timing. Current biology : CB *21*, 2055-2063.

Tanaka, S., Umemori, T., Hirai, K., Muramatsu, S., Kamimura, Y., and Araki, H. (2007). CDK-dependent phosphorylation of Sld2 and Sld3 initiates DNA replication in budding yeast. Nature *445*, 328-332.

Figure S1

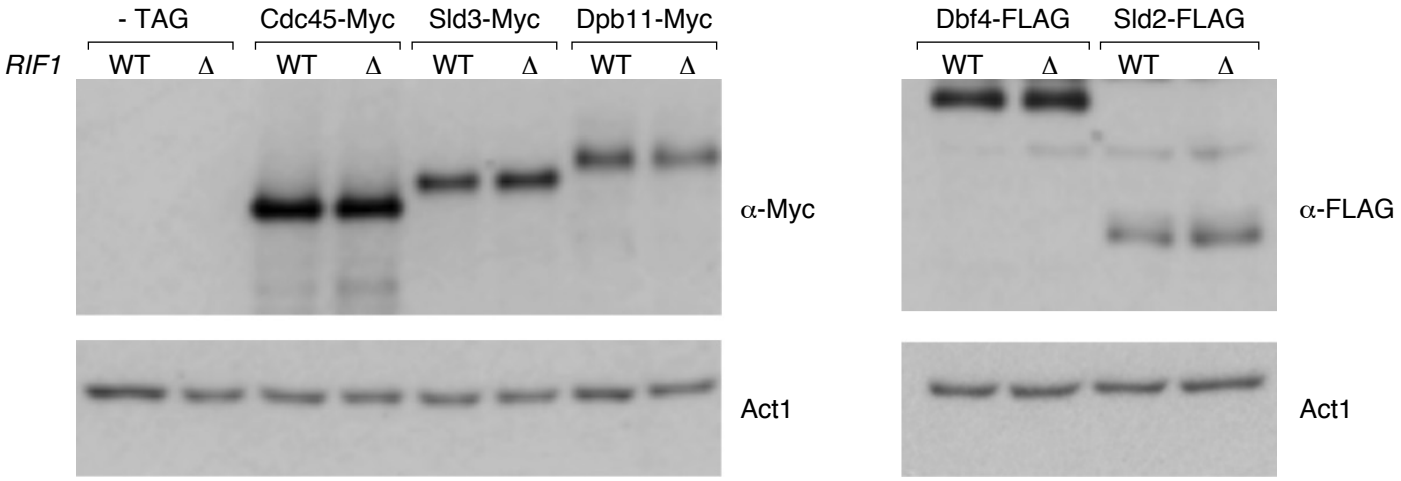
- TAG
Cdc45-Myc
Sld3-Myc
Dpb11-Myc
Dbf4-FLAG
Sld2-FLAG
RIF1
WT
Δ
WT
Δ
WT
Δ
WT
Δ
WT
Δ
WT
Δ
α-Myc
α-FLAG
Act1
Act1

Figure S2

A

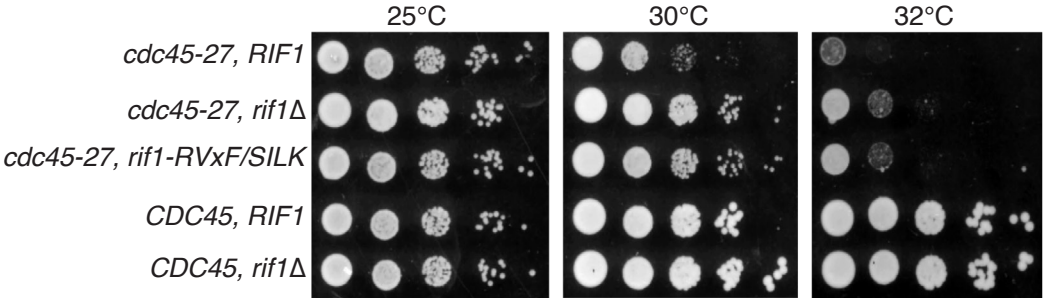
25°C
30°C
32°C
cdc45-27, RIF1
cdc45-27, rif1Δ
cdc45-27, rif1-RVxF/SILK
CDC45, RIF1
CDC45, rif1Δ

B

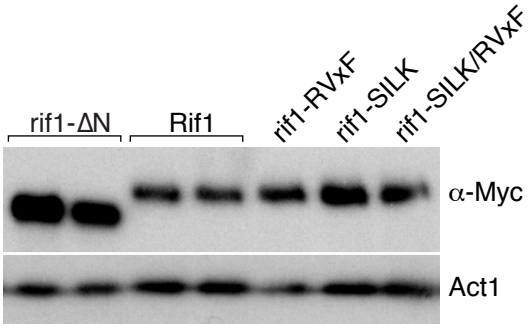
rif1-ΔN
Rif1
rif1-RVxF
rif1-SILK
rif1-SILK/RVxF
α-Myc
Act1

Figure S3

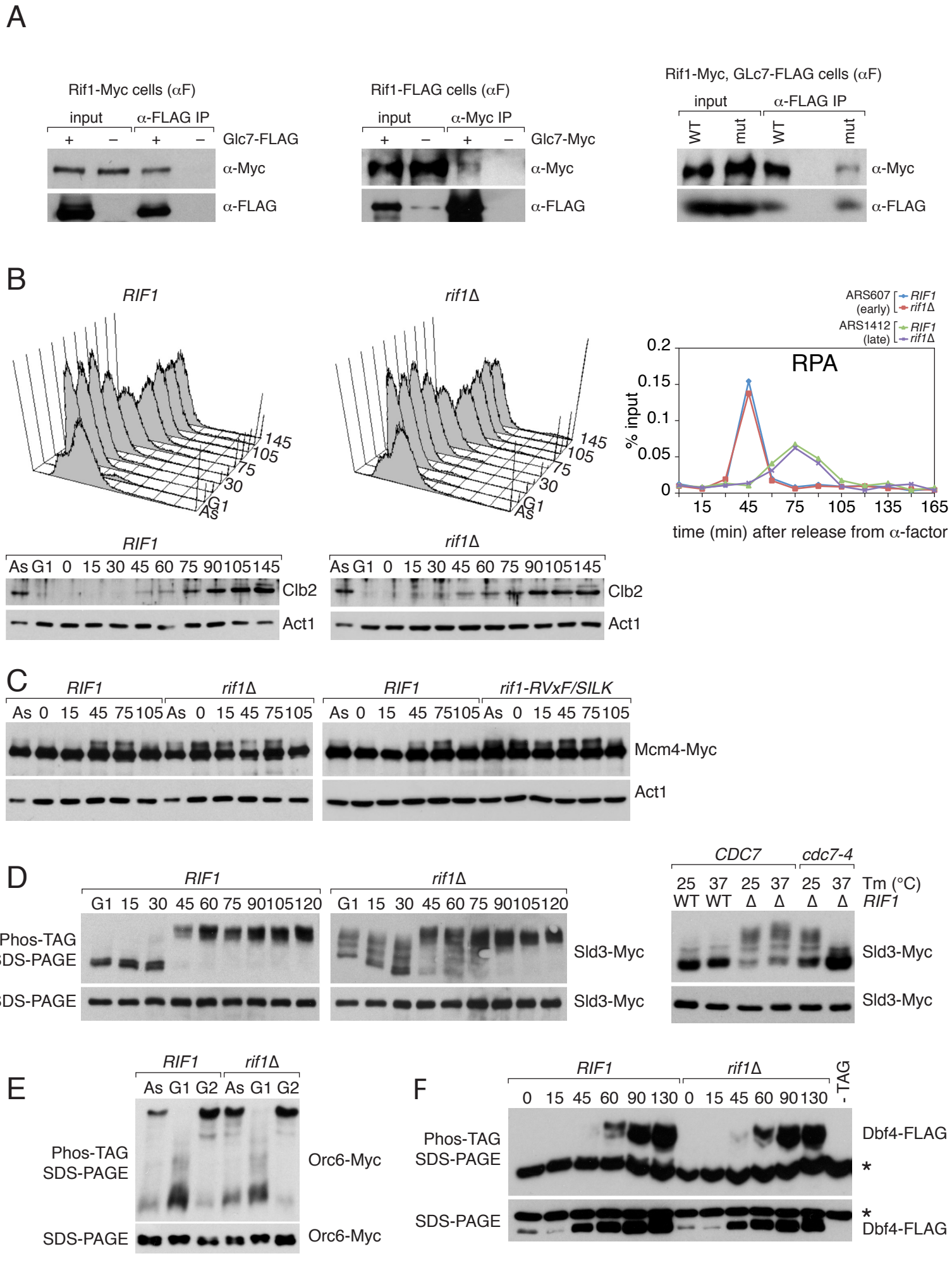
A
Rif1-Myc cells (αF)
input
α-FLAG IP
+ − + −
Glc7-FLAG
α-Myc
α-FLAG
Rif1-FLAG cells (αF)
input
α-Myc IP
+ − + −
Glc7-Myc
α-Myc
α-FLAG
Rif1-Myc, GLc7-FLAG cells (αF)
input
α-FLAG IP
WT mut WT mut
α-Myc
α-FLAG
B
RIF1
rif1Δ
As
G1
30
75
105
145
ARS607 (early) RIF1 rif1Δ
ARS1412 (late) RIF1 rif1Δ
RPA
% input
0.2
0.15
0.1
0.05
0
15 45 75 105 135 165
time (min) after release from α-factor
RIF1
rif1Δ
As G1 0 15 30 45 60 75 90 105 145
Clb2
Act1
C
RIF1
rif1Δ
rif1-RVxF/SILK
As 0 15 45 75 105
Mcm4-Myc
Act1
D
RIF1
rif1Δ
G1 15 30 45 60 75 90 105 120
Phos-TAG SDS-PAGE
SDS-PAGE
Sld3-Myc
CDC7
cdc7-4
25 37 25 37 25 37 Tm (°C)
WT WT Δ Δ Δ Δ RIF1
E
RIF1
rif1Δ
As G1 G2 As G1 G2
Phos-TAG SDS-PAGE
SDS-PAGE
Orc6-Myc
F
RIF1
rif1Δ
0 15 45 60 90 130 0 15 45 60 90 130 - TAG
Phos-TAG SDS-PAGE
SDS-PAGE
Dbf4-FLAG
*

Figure S4

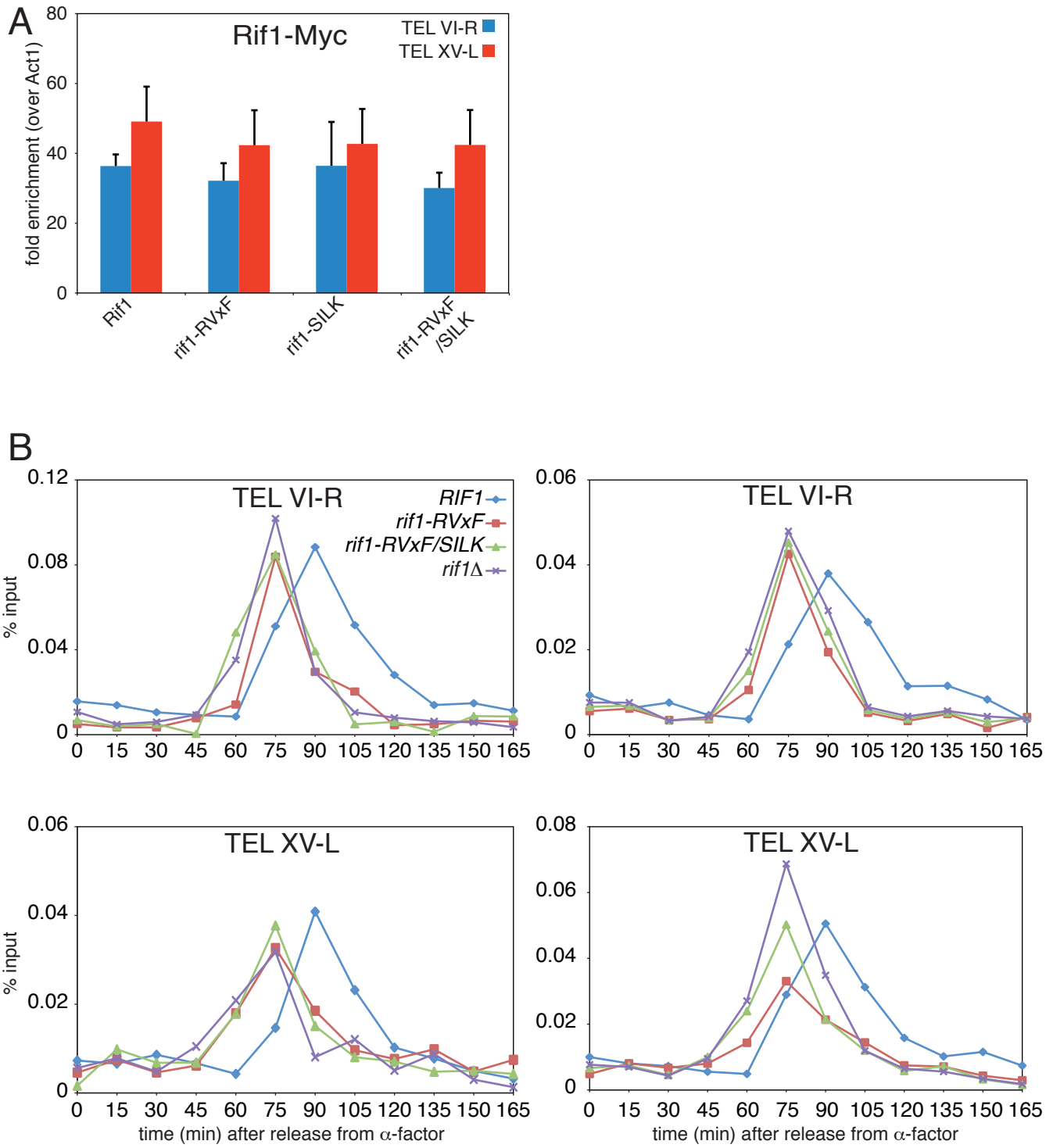
A
Rif1-Myc
TEL VI-R
TEL XV-L
fold enrichment (over Act1)
0
20
40
60
80
Rif1
rif1-RVxF
rif1-SILK
rif1-RVxF /SILK
B
TEL VI-R
RIF1
rif1-RVxF
rif1-RVxF/SILK
rif1Δ
% input
0.12
0.08
0.04
0
0.06
0.02
0 15 30 45 60 75 90 105 120 135 150 165
TEL XV-L
0.08
0.06
time (min) after release from α-factor